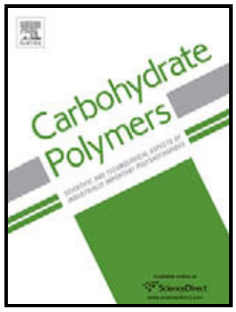

Title: A study of the structural changes in a chitosan matrix produced by the adsorption of copper and chromium ions

Authors: Pablo S. Anbinder, Carlos Macchi, Javier Amalvy, Alberto Somoza

PII: S0144-8617(19)30647-2
DOI: https://doi.org/10.1016/j.carbpol.2019.114987
Article Number: 114987

Reference: CARP 114987

To appear in:

Received date: 14 March 2019
Revised date: 7 June 2019
Accepted date: 7 June 2019

Please cite this article as: Anbinder PS, Macchi C, Amalvy J, Somoza A, A study of the structural changes in a chitosan matrix produced by the adsorption of copper and chromium ions, *Carbohydrate Polymers* (2019), https://doi.org/10.1016/j.carbpol.2019.114987

A study of the structural changes in a chitosan matrix produced by the adsorption of copper and chromium ions

Pablo S. Anbinder[1,*], Carlos Macchi[1], Javier Amalvy[2,3] and Alberto Somoza[1]

[1]Instituto de Física de Materiales Tandil - IFIMAT (UNCPBA) and CIFICEN (UNCPBA-CICPBA-CONICET), Pinto 399, (B7000GHG) Tandil, Argentina.

[2]Instituto de Investigaciones Físico-Químicas Teóricas y Aplicadas (INIFTA) - (CONICET CCT La Plata-UNLP), Diag. 113 y 64, 1900 La Plata, Argentina.

[3]Centro de Investigación y Desarrollo en Ciencia y Tecnología de Materiales (CITEMA) – (UTN – CICPBA). Av. 60 y 124, 1900 Berisso, Argentina.

[*] **Corresponding author:** anbinder@exa.unicen.edu.ar, phone: ++54 249 438-5670 Int. 2854, Pinto 399, (B7000GHG) Tandil, Argentina.

Highlights

- Structural mechanisms operating in metal ion-adsorbed chitosan matrices are discussed
- Interaction between Cu(II) and CS mainly occurs via NH_2 groups in a pendant fashion
- Cr (VI) species interact with both -NH_2 and -OH chitosan functional groups
- The nanostructure of the adsorbed CS depends on the metal ion-matrix interactions

ABSTRACT

A study of the structural changes at micro- and nano-scale in a chitosan matrix after the adsorption of different metal ions is presented. Toward this aim, samples of chitosan films soaked in different concentrations of copper(II) and chromium(VI) aqueous solutions were prepared. Cu and Cr ions were selected as sorbates since they have different ionic properties. The effect of the adsorbed metal ions on the microstructure of the chitosan matrices were studied using Fourier transformed infrared spectroscopy, UV-visible spectroscopy, differential scanning calorimetry and thermogravimetric analysis. To go further into the study of the samples at the molecular level, the

nuclear technique positron annihilation lifetime spectroscopy was used. Results are discussed in terms of the interaction between the metal ions and the chitosan functional groups.

KEYWORDS: CHITOSAN, POSITRON ANNIHILATION SPECTROSCOPY, HEAVY METAL ADSORPTION, STRUCTURAL PROPERTIES

1. Introduction

Biosorption is an emerging area in which heavy metals are adsorbed and retained by biomaterials. The principal advantages of this adsorption area include biocompatibility, biodegradability, price affordability with high effectiveness, minimum usage of chemicals, restoration of biosorbent and possible usage of recovered metal (Ali and Gupta, 2007; Nithya *et al.*, 2016). Among biomaterials, biopolymers are especially used as heavy metal removals due to their proved ability to bind transition metals. One of the most studied biopolymer in this area is the polysaccharide known as chitosan (CS). This polymer is the partially deacetylated form of the chitin, a natural polysaccharide extracted from crabs, shrimps and other crustaceans' exoskeleton. In general, chitosan occurs as N-acetylglucosamine and N-glucosamine copolymer that are randomly or block distributed throughout the biopolymer chain (Muzzarelli, 1973; Rinaudo, 2006).

Chitosan has been widely studied as metal ion sorbent due to its high adsorption potential, which could be related to its high hydrophilicity, the presence of functional groups (-OH and $-NH_2$) in its structure with proved affinity to metals, and the flexible structure of this biopolymer (Muzzarelli, 1973). Among different applications, the effectiveness of the use of CS matrices in capture and removal of metal pollutants for wastewater treatments was recently discussed (Li *et al*., 2016; Olivera *et al*., 2016). On this issue, there still remain different open questions as from the fundamental research as the technological applications.

Most of the studies dedicated to the characterization of CS and CS-heavy metal ion complexes were carried out using conventional techniques which mainly make it possible to get structural and morphological information up to the microscale. But, nanostructural studies of these systems are still scarce, due to the lack of suitable probes for molecular dimensions (Xia *et al.*, 2016). The size and distribution of the free volumes (*i.e.*, the non-occupied volumes) in a polymer matrix confer different properties to polymers; that is, differences in the mechanical (Ray, Galy, Sautereau, Simon and Cook, 2004), thermal (McCullagh, Yu, Jamieson, Blackwell and McGerve, 1995) and barrier (Zekriardehani, Jabarin, Gidley and Coleman, 2017) properties. Free volume is one of the key parameters in determining the molecular mobility of the polymeric segments. Positron Annihilation Lifetime Spectroscopy (PALS) has proven to be an excellent tool to detect changes at nanoscale in polymeric materials (Jean, 1990). It is due to its particular sensitivity to small holes and free volumes of the order of angstrom magnitude. PALS is the only analytical technique that makes it possible to directly obtain the size and concentration of the free nanohole volumes of porous materials (Jean, Mallon and Schrader, 2003).

It is important to point out that the precise binding mechanism between the metal ions and the CS matrix is still being debated, due to the variety of the mechanisms of chelation and the possibility of ion exchange (see for example Rhazi *et al.*, 2002; Skoric *et al.*, 2005; Bratskaya *et al.*, 2013). In our laboratory, we are carrying out a general study addressed to understand the processes and mechanisms responsible for structural changes at the micro- and nano-scale of the chitosan matrix after the adsorption of different metal ions. This kind of studies provides valuable information about the nature of the metal-chitosan

interactions, useful for the design of more effective biopolymeric systems with potential application in the environmental protection field.

This work is particularly focused on the study of the interaction between two different metal ions with the chitosan functional groups, Cu (II) and Cr (VI). These metal ions were chosen because both present well-differentiated ionic properties when they are dissolved in aqueous solution; that is, Cu (II) is a metal cation existing in aqueous solutions as a hexaaquo complex and Cr (VI) can exist as oxoanions species. This behavior can modify substantially the interaction with the amino and hydroxyl groups of CS; for example, in the case of chromium ion species the metal center is already fully coordinated by oxygens. (Wilkins, 2002). So a detailed analysis on the chemical behavior of the ionic species interacting with the CS matrix is relevant when a correlation between the structural changes at nanoscale and the adsorption of the different metal ions is discussed.

2. Materials and Methods

2.1. Materials

The materials and chemicals used in this work were medium molecular weight chitosan (CS) with 95.2% deacetylation degree and M_v 310,000, provided by Parafarm (Argentina); and metal salts ($CuSO_4.5H_2O$ and $K_2Cr_2O_7$) were supplied by Fluka AG (Switzerland). All reagents were of analytical grade and were used without purification. Chitosan M_v was determined by capillary viscosimetry and DD% was obtained by FT-IR (Baxter, Dillon, Taylor and Roberts, 1992) and confirmed by potentiometry (Jiang, Chen, and Zhong, 2003).

2.2. Methods

2.2.1 Films preparation

Chitosan films were prepared by casting in Petri dishes from stock solutions of 2% w/v of chitosan in acetic acid 1% v/v. After drying for 24 h at 40 °C, films were neutralized with NaOH 1M, rinsed with distilled water and dried again for 48 h at 40 °C. Films were kept at room temperature (RT, 25 °C) in a desiccator with silica gel until use. After drying, films thicknesses were typically about 100 µm.

2.2.2 Metal ion sorption

Metal sorption was performed by soaking of 0.8 g of dry CS films with 1 L of solution containing different concentrations of metal ions. The experiments were carried out in conical flasks at RT and for 24 h. Under these experimental conditions the equilibrium state of all systems is reached.

The pH was adjusted to 7 using hydrochloric acid and sodium hydroxide molar solutions. It was reported that the pH of the solution has a strong influence on the adsorption capability of the sorbent (Nithya *et al.*, 2016; Kyzas, Kostoglou and Lazaridis, 2009; Elwakeel & Guibal, 2015). Therefore, to avoid structural modifications of the matrix due to different protonation, the same pH value was chosen for both Cu(II) and Cr(VI) solutions. It is known that Cu(II) precipitates mostly as copper hydroxide at intermediate pH levels, but it is dependent on the copper concentration (*Cuppett, Duncan and Dietrich, 2006*). In our case, the maximum concentration used was 2.36 mM which is below the threshold concentration for which precipitation effect can be detected.

2.2.3 Metal adsorption quantification

Metal ion concentration in solutions was determined by flame atomic absorption spectroscopy (AAS) using a Shimadzu AA6800 instrument. Once time elapsed, films were retired from the solutions and the pH were lowered to a pH 2 with nitric acid to solubilize any precipitates.

2.2.4 UV-visible spectroscopy

UV-vis absorption spectra of the films (100 µm thickness) were obtained using a Shimadzu SPD-10AVP UV-vis. spectrophotometer in a wavelength range from 200 to 800 nm.

2.2.5 Fourier Transformed Infrared spectroscopy

FT-IR spectra of films were acquired in the transmission mode using a FT-IR Nicolet 380 spectrometer, taking 64 scans per spectra, with a resolution of 4 cm^{-1}. Films were previously immersed in liquid nitrogen, milled and mixed with spectroscopic KBr to obtain disks.

2.2.6 Differential scanning calorimetry and thermogravimetric analysis

DSC studies were performed in a TA-Q20 calorimeter. Thermograms were acquired at 10 °C/min from 20 °C to 450 °C with Ar purge (50 mL/min). Before measurements, the samples were maintained for 48 h in a desiccator with silica gel at RT. TGA curves were obtained using a Shimadzu DTG-60 analyzer, running about 10 mg sample from RT to 600 °C at a heating rate of 10 °C/min with N_2 purge (30 mL/min).

2.2.7 Positron annihilation lifetime spectroscopy

The positron lifetime spectrometer used consisted of a "fast–fast" coincidence system with a resolution of 330 ps. PALS spectra were recorded at RT with a total number of 1.5×10^6 coincidence counts using a 0.2 MBq sealed source of $^{22}NaCl$ deposited onto a thin Kapton foil (1.08 mg/cm^2). The source was sandwiched between two "identical pieces" of the sample material. At least five measurements were taken for each film sample. The experimental set-up was previously described in Anbinder, Macchi, Amalvy and Somoza (2016).

According to the common interpretation for PALS measurements in polymers, spectra were deconvoluted into three discrete lifetime components using the LT10 software (Giebel & Kansy, 2011). As usual, the longest lifetime component τ_3 is attributed to the ortho-Ps decay in the nanoholes forming the free volume; that is, $\tau_3 = \tau_{o\text{-}Ps}$. The intermediate component τ_2 (0.35 – 0.50 ns) is attributed to positrons annihilated in low electron density regions of the structure. The shortest component τ_1 (0.1– 0.2 ns) is due to positrons annihilated into the bulk and to para-Ps annihilations.

2.2.8 Samples nomenclature

While chitosan film was named as CS, adsorbed films were named according to the metal ion and its concentration on the initial solution. For instance, samples soaked in solutions containing 80 mg Cu/L or 20 mg Cr/L were labeled as Cu80 and Cr20, respectively.

3. Results and discussion

Metal ion adsorption

The first insight of metal adsorption is the change in color films. Depending on the concentration of the adsorbed metal ion, the films containing Cr(VI) changed from pale yellow to different tones of

brown; in the Cu(II)-adsorbed films different tones of the green-blue color were observed. Similar findings were reported by Ferrero, Tonetti and Periolatto (2014) for chitosan-coated cotton gauze.

Sorption capacity values for the different samples are reported in Table 1. The highest values of each initial metal ion solution concentration (C_0) were chosen on the base that beyond these concentrations the films became too brittle to be manipulated. Depending on the metal ion, solutions with lower C_0 values were also prepared; specifically, samples soaked in a solution containing 0.38 mM of Cr (sample Cr20) and 1.26 mM of Cu (sample Cu80). The sample Cu80 was specifically prepared in order to establish a comparison of the morphological properties between the Cu and Cr-adsorbed films with similar initial metal ion solution concentration.

As can be seen in Table 1, there exist clear differences in the adsorption of the metal ions by the chitosan films in the conditions above-described. The sorption capacity values measured in this work are in good agreement with those reported in studies of heavy metal ions adsorption by chitosan (Schmuhl, Krieg and Keizer, 2001; Bailey, Olin, Bricka and Adrian, 1999; Giraldo, Rivas, Elgueta and Mancisidor, 2017).

As can be observed in Table I, an increase of the C_0 values is replicated in an increment of the corresponding sorption capacity values. A similar behavior was reported by Giraldo, Rivas, Elgueta and Mancisidor (2017).

Table 1- Sorption capacity of metal ions by chitosan films

Metal ion	***C_0 (mg/L)***	***C_0 (mM)***	***C_1 (mM)***	***Concentration Difference (mM)***	***Sorption capacity (mmol/g)***
Cu(II)	80	1.26	0.31 ± 0.03	0.95	1.19 ± 0.06
	150	2.36	0.59 ± 0.04	1.77	2.22 ± 0.12
Cr(VI)	20	0.38	0.25 ± 0.01	0.14	0.17 ± 0.02
	80	1.54	0.98 ± 0.07	0.56	0.70 ± 0.04

*C_0 is the initial metal ion solution concentration; C_1 is the metal ion solution concentration after adsorption; Sorption capacity is the amount in mmol of metal ion adsorbed by gram of chitosan.

Differences between metal ions adsorption by chitosan had been explained by the different permeability of the sorbates through the chitosan matrix (sorbent), which is also related to the metal ion-chitosan affinity (Krajewska, 2001). On the other hand, in a study of Pb(II) and Cu(II) adsorption by chitosan, Deans & Dixon (1992) assigned the differences in the sorption capacity to the metal ion sizes.

As a first result from the data reported in Table 1, it can be concluded that for those samples with similar C_0 the sorption capacity value of the Cu-adsorbed samples is about 70% higher than that obtained for the Cr absorbed samples.

UV-visible spectroscopy

In Fig. 1, the UV-visible spectra for the samples CS, Cu80 and Cr80 are shown. For chitosan films three bands at 245, 315 and 385 nm are observed.

Previous to analyze and discuss the spectra of chitosan films containing metal ions, we consider important to describe which are the main features of the possible metal species that could be present in the aqueous solutions. In the case of copper, Cu(II) ions are present as the aquocomplex $[Cu(H_2O)_6]^{2+}$. On the other hand,

chromium(VI) exists as $Cr_2O_7^{2-}$, $HCrO_4^-$, CrO_4^{2-} and $HCr_2O_7^-$ depending upon the ionic concentration and pH of the solution (Balakrishna Prabhu, Saidutta and Srinivas Kini, 2017). It has been reported that for pH 7 the main species of Cr(VI) present in the solution are CrO_4^{2-}, $HCrO_4^-$ and $Cr_2O_7^{2-}$ (Fournier–Salaun and Salaun, 2007). But, $Cr_2O_7^{2-}$ anions are only present at a high Cr (VI) concentration (>1000 ppm) (Balakrishna Prabhu, Saidutta and Srinivas Kini, 2017). At low chromium concentration (<100 ppm), the main fraction is $HCrO_4^-$ with pH below 5, whereas the CrO_4^{2-} increases with the increase of pH value becoming the main form for a pH above 7 (Qin *et al.*, 2003). Therefore, as our solutions were prepared with pH 7 and with very low Cr concentration (< 80 ppm) the main species of Cr(VI) are $HCrO_4^-$ and CrO_4^{2-}. It is well known that the electronic spectrum of $HCrO_4^-$ presents two bands at 260 and 350 nm and a shoulder at 290 nm; and for the chromate ion, the electronic transitions in the near UV-visible spectrum are observed at 303, 387 and 450 (weak) nm. In the literature, the described bands were assigned to $^1A_1 \rightarrow {}^1T_2$ ($3t_2 \rightarrow 2e$), $^1A_1 \rightarrow {}^1T_2$ ($t_1 \rightarrow 2e$) and $^1A_1 \rightarrow {}^1T_1$ ($t_1 \rightarrow 2e$) transitions, respectively (see *Johnson and McGlynn, 1970)*.

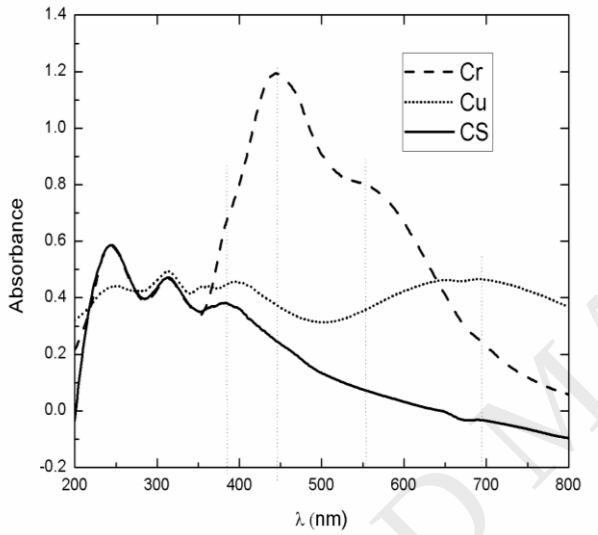

Figure 1 - UV-visible spectra for the samples CS, Cu80 and Cr80.

As can be observed in Fig. 1, the UV-visible spectra corresponding to the metal ion-adsorbed samples present additional bands with respect to those observed for CS. In the UV-vis spectrum for the sample Cr80 a band at 450 nm and two shoulders at 380 and 550 nm are observed. The shoulder at 380 nm could mainly be assigned to the presence of the CrO_4^{2-} ion in the chitosan matrix, but some contribution from the $HCrO_4^-$ could not be discarded. Although weak in the pure species, the band at 450 nm presents an important increase in its intensity when the metal ion is adsorbed in the chitosan matrix. In such a case, the Cr-O bonds involved in the interaction with the matrix are disturbed; this effect should diminish the ion symmetry modifying the intensities of the bands. The presence of a shoulder around 550 nm has not been previously reported for Cr ion adsorbed chitosan films. However, a contribution to the mentioned shoulder coming from some electronic transitions of Cr(III) ion species could not be discarded. In this sense, Shen *et al.* (2013) and Guibal, Dambien, Guimon and Yiacumi (2001) concluded that a small portion of the Cr(VI) bound to the chitosan matrix can be reduced to Cr(III).

In the case of Cu80 sample, the UV-vis. spectrum presents a broad band starting at 500 nm with a maximum at 680 nm. This band can be attributed to the d–d transitions of Cu(II) complexes formed with functional groups of the chitosan matrix (Bell, 1981).

Infrared spectroscopy

As can be seen in Fig. 2, the IR spectrum of chitosan shows characteristic absorption bands at 3362 cm^{-1} assigned to the overlapped OH and NH stretching vibrations and 2927 cm^{-1} and 2880 cm^{-1} due to C-H stretching vibration of CH and CH_2 groups. Additionally, two peaks at 1642 cm^{-1} and 1564 cm^{-1} corresponding to amide bending are observed. The former (named Amide I) came from N–H and the second peak (named Amide II) from NH_2. Finally, the band at 1075 cm^{-1} was assigned to the C-O stretching vibration of the primary alcohol (Anbinder *et al.*, 2016).

When comparing to the IR spectrum of chitosan, those of metal ion-adsorbed films present different shifts in the wavenumber of the bands assigned to the functional groups of the polymer. Specifically, in the FT-IR spectrum obtained for the sample Cr80, the band at 3362 cm^{-1} shifted to 3420 cm^{-1} and the maximum of the Amide II band shifted from 1564 cm^{-1} to 1600 cm^{-1} and became broader. Due to the width of this band, it is not possible to define the position of the Amide I peak. Furthermore, the band assigned to C-O stretching of the primary alcohol slightly shifted to higher wavenumbers (from 1075 cm^{-1} to 1084 cm^{-1}) and became broader compared with the same band in the pure chitosan spectrum. The changes observed reveal important interactions between Cr ions with N, and also with O atoms of the chitosan. These results are in agreement with those reported by Vieira *et al.* (2014), who studied Cr-chitosan complexes using EXAFS/XANES.

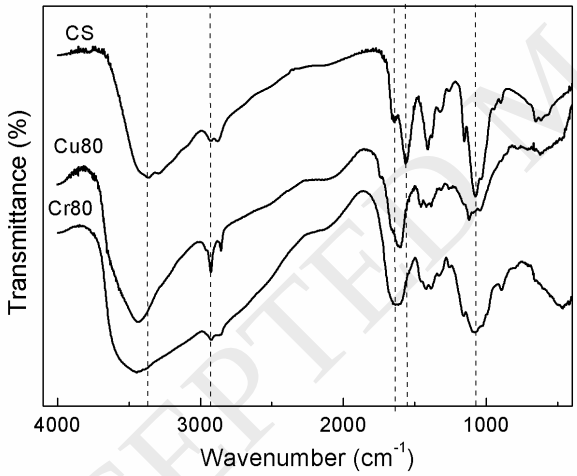

Figure 2 - FT-IR spectra for the samples CS, Cu80 and Cr80.

In the case of sample Cu80, the bands assigned to NH functional groups change when comparing to that of CS. Specifically, the broad band centered at 3362 cm^{-1} shifted to 3415 cm^{-1}. Furthermore, the maximum of the Amide II band shifted to 1610 cm^{-1} and the Amide I band appear as a shoulder at 1650 cm^{-1}. In the same spectrum, the band at 1075 cm^{-1} has a marked change in its intensity when comparing to that of the CS. However, this change cannot be uniquely assigned to the formation of CS-Cu coordinated links through the hydroxide groups. In fact, it must also be taken into account that around the same wavenumber there exists the υ_4 mode of the free $(SO_4)^{2-}$ ion coming from copper sulphate as well (Ferraro and Walker, 1965).

Differential Scanning Calorimetry and Thermogravimetric Analysis

In Fig. 3, DSC thermograms corresponding to pure chitosan and metal ion adsorbed films are shown.

In the curve obtained for CS, an endothermic peak around 110-150 °C and an exothermic peak around 300 °C are observed, both in good agreement with results reported in the literature (Coelho, Laus, Mangrich, de Fábere and Larqanjeira, 2007; Trimukhe & Varma, 2009). As usual, the endothermic peak is assigned to water removal and the exothermic one to the chitosan thermal degradation.

In the case of metal ion adsorbed films, the thermograms obtained for the samples Cu80 and Cr80 show that the endothermic event is slightly shifted to a lower temperature (from ~135 °C to ~130 °C) and in both cases it is sharper than that corresponding to the pure chitosan. As can be seen in the figure, the exothermic peaks are also shifted when comparing with that obtained for the CS. Specifically, the exothermic peak of the sample Cu80 is significantly shifted to a lower temperature (from ~300 °C to ~240 °C), on the contrary for the sample Cr80 this peak is slightly shifted toward a higher temperature (from ~300 °C to ~310 °C).

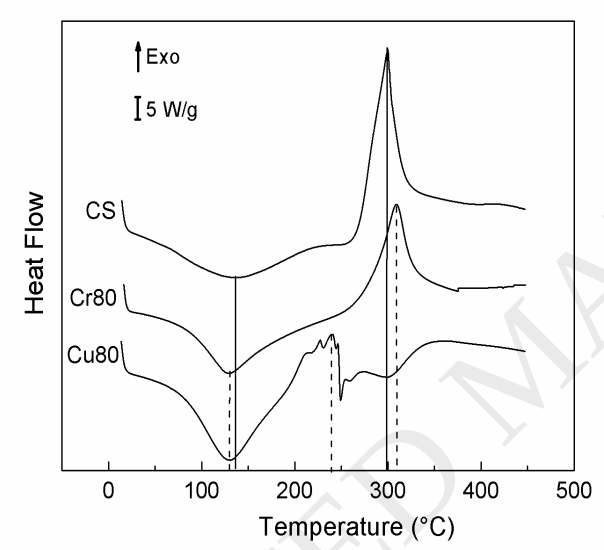

Figure 3 - DSC thermograms for the samples CS, Cr80 and Cu80.

The shift of the exothermic peak in the sample Cu80 could be attributed to the interaction between the adsorbed Cu ions and the chitosan amino groups. It was reported that such functional groups are the responsible for the structural stability of the CS matrix (Tirkistani, 1998). A similar temperature decrease of the exothermic peak for metal ion-chitosan complexes was reported for those complexes in which metal ions are only associated with chitosan through the amino groups (Trimukhe & Varma, 2009). There are several studies on the mechanisms involved in the sorption of copper ions by the chitosan matrix; but they are not still fully understood (Rhazi *et al.*, 2002, Skorik *et al.*, 2005). Although it is generally accepted that the free amino group is mainly involved in the coordination with metal ions, in the literature there are controversial conclusions based on experimental and theoretical evidences with respect to the structure of the formed complexes, mainly the participation or not of hydroxyl groups in the metal coordination (Terreux, Domard, Viton and Domard, 2006; Bratskaya *et al.*, 2013; Skorik *et al.*, 2005).

The formation of the mentioned complexes were described using two different models (Schlick, 1986; Ogawa, Oka and Yui, 1993). In the first one, named “bridge model”, copper ions are bound to

several amine groups from the same chain or from different chains, via inter- or intra-molecular complexation. The second model is known as “pendant model”, in which the metal ion is bound to an amine group in a pendant fashion, forming a unique complex with copper whose structure is close to $[CuNH_2(OH)_2]$ (Guibal, 2004). The fourth site of the coordination sphere of copper can be occupied by a water molecule. Although the most favorable coordination model – “bridge” or “pendant” – is still disputable, it has been reported (Lü, Cao and Shen, 2008; Skorik *et al.*, 2005) that under certain experimental conditions one or another model could be used to describe the formation of complexes (Bratskaya *et al.*, 2013).

In the case of Cr-adsorbed films, the shift to higher temperatures of the exothermic peak indicates that a higher energy than that for the pure chitosan matrix is necessary for the thermal degradation of the films. In total agreement with the analysis of FT-IR spectra, this experimental evidence can be interpreted in terms of the coexistence of two kinds of interactions among the Cr ions with the CS matrix; that is, the amine groups and the hydroxyl groups. The balance of the effects resulting from both kinds of interactions gives the Cr ion-CS complexes a higher thermal stability, and therefore structural, than that of the CS.

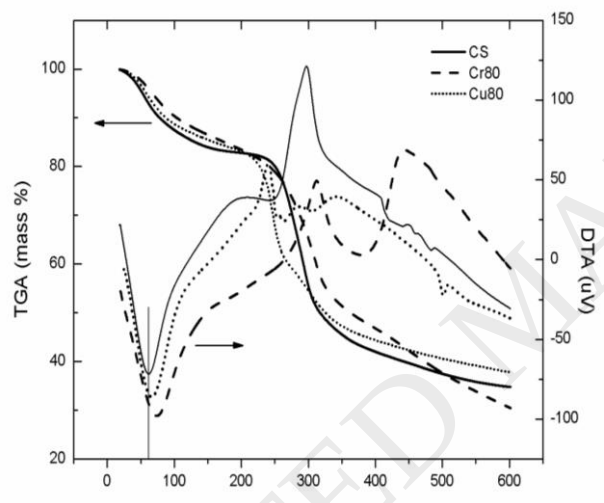

Figure 4 - TGA and DTA curves for the CS, Cu80 and Cr80 samples.

In Fig. 4, TGA and DTA curves for the CS and the samples Cr80 and Cu80 are shown. For all samples, the evolution of TGA curves presents two well-defined stages. In the first one, the mass loss is similar for pure CS as well for metal ion adsorbed samples (~17 wt. %) and can be attributed to the water removal. In the same stage, from the analysis of the DTA curves it results that the shifts of the temperatures at the maximum rate T_{max} with that of CS matrix depend on the adsorbed metal ion. In fact, for Cu80 T_{max} increases from 62 °C to 66 °C; this temperature increment is more marked for sample Cr80 (from 62 °C to 74 °C). The higher energy required for the water removal in both Cr and Cu-adsorbed films with respect to pure chitosan suggests that water molecules are in the coordination sphere of metal ions together with groups of chitosan. The higher T_{max} value in Cr-adsorbed samples with respect to Cu ones could be explained in terms of an increase of the number of interaction points between the metal ion and the chitosan.

It is worth mentioning that the T_{max} values corresponding to the second stage in the DTA curves, assigned to chitosan degradation are in very good agreement with the exotherms observed in the DSC

thermograms presented in Fig. 3. That means that both TGA and DTA results can be interpreted in the same terms as those used in the analysis of DSC results.

Positron annihilation lifetime spectroscopy (PALS)

In Table 2 results of the o-Ps lifetimes $\tau_{o\text{-}Ps}$ are presented. The values obtained for pure chitosan are in good agreement with those reported in the literature (Sharma *et al.*, 2013; Chaudhary, Went, Nakagawa, Buckman and Sullivan, 2010).

The nanoholes radii R were obtained using a simple quantum mechanical model (Tao, 1972; Eldrup, Lightbody and Sherwook, 1981). This model makes it possible to correlate the longest lifetime component $\tau_3 = \tau_{o\text{-}Ps}$ with R by means of the following equation:

$$\tau_{o-Ps} = 0.5\left[\frac{\Delta R}{R+\Delta R} + \frac{1}{2\pi}\sin\left(\frac{2\pi R}{R+\Delta R}\right)\right]^{-1} \qquad \text{Eq. (1)}$$

Where $\tau_{o\text{-}Ps}$ is given in ns, R in nm and ΔR = 0.166 nm (Nakanishi, 1988). Then, the corresponding free nanohole volume v_h is obtained using Eq. (2); that is,

$$v_h = \frac{4}{3}\pi R^3 \qquad \text{Eq. (2)}$$

Table 2– ortho-Positronium lifetimes, holes radii and free volumes obtained from the analysis of PALS spectra in pure chitosan and samples soaked in metal ions solutions.

Sample	$\tau_{o\text{-}Ps}$ (ps)	R* (Å)	v_h* (Å^3)
CS	1650 ± 10	2.51	66.2
Cu80	1500± 20	2.34	53.7
Cu150	1450 ± 20	2.28	49.6
Cr20	1335 ± 20	2.15	41.6
Cr80	1265 ± 20	2.05	36.1

*Hole radius (R) and the corresponding free volume (v_h) values were obtained using Eqs. (1) and (2), respectively.
*Typical errors associated with *R* and v_h values are lower than 2 %.

The evolution of v_h as a function of the initial metal ion solution concentration for Cu and Cr is presented in Fig. 5. As can be seen, the free nanohole volume value obtained for the CS matrix is higher than those for all the metal ions adsorbed samples. In the case of Cu-adsorbed samples, an almost linear decrease of v_h for increasing C_0 is observed. On the other hand, for the Cr-adsorbed samples a strong decrease of v_h is observed for an initial concentration as lower as 0.38 mM; for a higher concentration, v_h presents a slight decrease

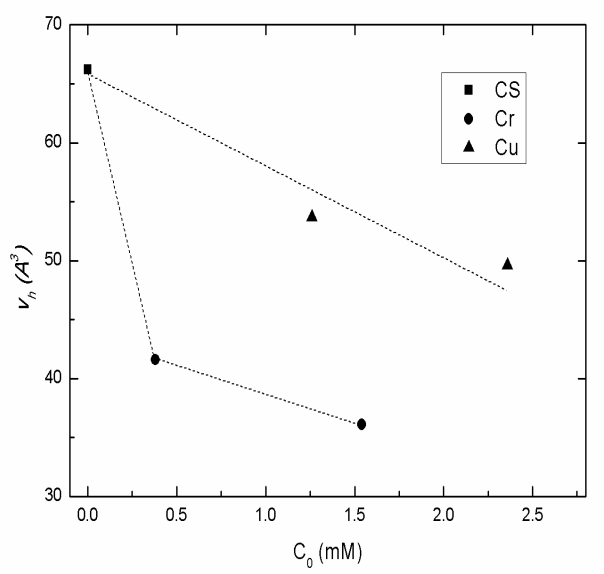

Figure 5 - v_h values for CS and metal ion-adsorbed samples at different metal concentrations. Dash lines are only eye guides.

The described results indicate that, at the nanoscale, the CS matrix is more affected by the type of metal ion adsorbed than by its concentrations. Furthermore, it is important to point out that PALS results give a direct evidence on the changes occurring at molecular level in the CS matrix after the adsorption of each metal ion.

In particular, it can be concluded that the small size of the nanoholes in the CS matrix after the adsorption of Cr is consistent with a decrease of the polymer chains mobility produced by the inter- and intra-chain interactions generated into the matrix. PALS results jointly analyzed with those obtained by DSC and FT-IR indicate that the operating mechanism in the CS matrix is the result of multiple interactions among the Cr ions with both the amine and the hydroxyl functional groups of chitosan.

On the other hand, when Cu is the adsorbed ion the size of the nanoholes into the CS matrix is systematically bigger than those of the Cr-adsorbed samples as a consequence of the formation of more flexible nanostructures. In this case, all the experimental results reported in the present work point out that the Cu ion- CS matrix interaction can be well described under the frame of the pendant model in which the Cu ion is bound to a unique-CS amine group.

4. Conclusions

Results obtained from the study of the structural changes at micro- and nano-scale in a chitosan matrix after the adsorption of different concentrations of Cu (II) and Cr (VI) indicate that the biopolymeric matrix is more affected by the type of metal ion adsorbed than by its concentration. This behavior can be assigned to the different interactions occurring between metal ions and the chitosan matrix. Specifically, from the experimental evidences obtained in this work we can claim that:

(i) In Cu(II)-adsorbed films, the interaction between the metal ion and the chitosan matrix mainly occur via the amino groups in a pendant fashion.

(ii) In the case of Cr-adsorbed films, ion species interact with both amino and hydroxyl groups.

In order to illustrate the interplay between Cu and Cr ions with the chitosan matrix, we propose the following graphical description (see Fig. 6).

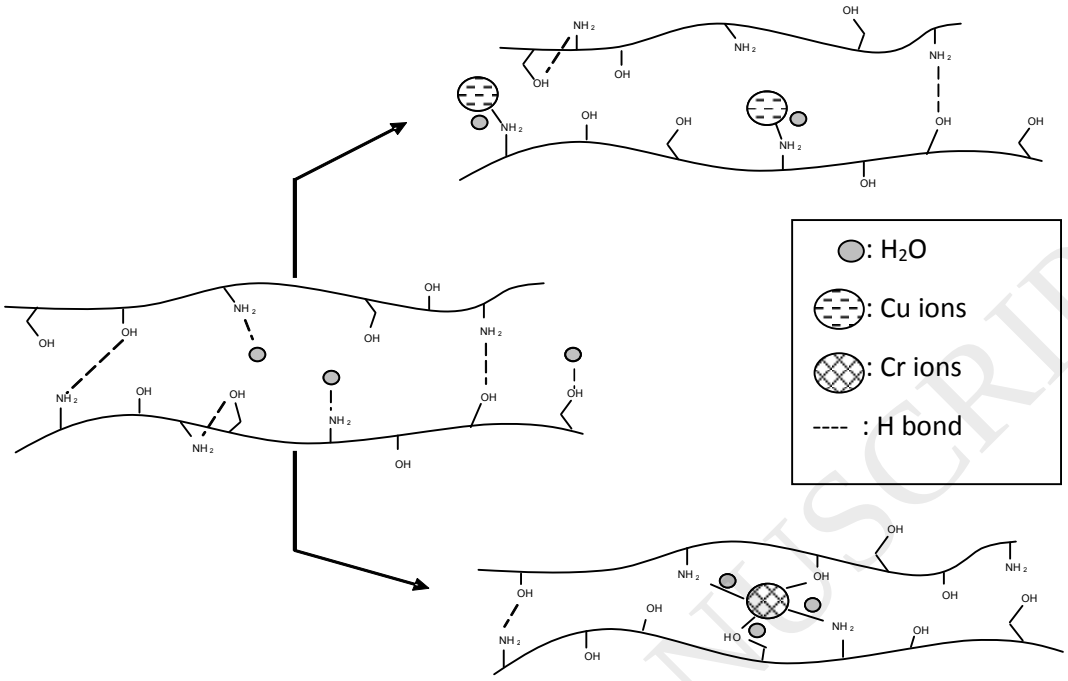

Figure - 6. Graphical description of the structure of the CS matrix and its metal ions complexes.

Acknowledgments

We acknowledge founding from the Agencia Nacional de Promoción Científica y Tecnológica (ANPCyT) PICT 2014-1785, PICT 2015-1068 and PICT 2015-1832; Consejo Nacional de Investigaciones Científicas y Técnicas; Comisión de Investigaciones Científicas de la Provincia de Buenos Aires; SECAT (UNCPBA) and Universidad Tecnológica Nacional.

4. References

Ali I. and Gupta V. (2007). Advances in water treatment by adsorption technology, *Nature Protocols* 1, pp 2661–2667.

Anbinder P., Macchi C., Amalvy J., Somoza A.(2016). Chitosan-graft-poly(n-butyl acrylate) copolymer: Synthesis and characterization of a natural/synthetic hybrid material. *Carbohydrate Polymers* 145, pp 86–94.

Bailey S., Olin T., Bricka M., Adrian D. (1999). A review of potentially low-cost sorbents for heavy metals. *Water Research* 33(11), pp 2469-2479.

Balakrishna Prabhu K., Saidutta M.B. and Srnivas Kini M. (2017). Adsorption of hexavalent chromium form aqueous medium using a new Schiff base chitosan derivative. *International Journal of Applied Engineering Research* 12(14) 4072-4082.

Baxter A., Dillon M., Taylor K. & Roberts G. (1992). Improved method for i.r determination of the degree of N-acetylation of chitosan. *International Journal of Biological Macromolecules*, 14, 166–169.

Bell J.E. (Ed.) (1981) Spectroscopy In Biochemistry, Volume 1, CRC Press.

Bratskaya S. Yu., Azarova Yu. A., Portnyagin A.S., Mechaev A.V., Voit A.V., Pestov A.V. (2013). Synthesis and properties of isomeric pyridyl-containing chitosan derivatives. *International Journal of Biological Macromolecules* 62, 426–432.

Chaudhary D., Went M.R., Nakagawa K., Buckman S.J. & Sullivan J. P. (2010). Molecular pore size characterization within chitosan biopolymer using positron annihilation lifetime spectroscopy. *Materials Letters*, 64, 2635–2637.

Coelho T., Laus R., Mangrich A., de Fávere A. and Laranjeira M. (2007). Effect of heparin coating on epichlorohydrin cross-linked chitosan microspheres on the adsorption of copper (II) ions. *Reactive & Functional Polymers* 67, pp. 468–475.

Cuppett J.D., Duncan S.E. and Dietrich A.M. (2006). Evaluation of Copper Speciation and Water Quality Factors That Affect Aqueous Copper Tasting Response*, Chem. Senses* 31, pp. 689–697

Deans J. and Dixon B. (1992). Uptake of Pb+2 and Cu+2 by novel biopolymers. *Water Research* 26(4), pp. 469-472.

Eldrup M., Lightbody D. & Sherwook N. J. (1981). The temperature dependence of positron lifetimes in solid pivalic acid. *Chemical Physics*, 63, 51–58.

Elwakeel K.Z. and Guibal E. (2015). Arsenic (V) sorption using chitosan/Cu(OH)2 and chitosan/CuO composite sorbents. *Carbohydrate Polymers* 134, pp 190–204.

Ferraro J.R. and Walker A. (1965). Comparison of the Infrared Spectra (4000-70 cm^{-1}) of several hydrated and anhydrous salts of transition metals. *J. Chem. Phys.* 42(4), pp 1278-1285.

Ferrero F., Tonetti C., Periolatto M. (2014). Adsorption of chromate and cupric ions onto chitosan-coated cotton gauze. *Carbohydrate Polymers* 110, pp 367-373.

Fournier–Salaun M-C. and Salaun P. (2007) Quantitative determination of hexavalent chromium in aqueous solutions by UV-Vis spectrophotometer. *Central European Journal of Chemistry* 5(4), pp. 1084–1093.

Giebel D. & Kansy J. (2011). A new version of LT program for positron lifetime spectra analysis. *Materials Science Forum*, 666, 138–141.

Giraldo J., Rivas B., Elgueta E., Mancisidor A. (2017). Metal ion sorption by chitosan-tripolyphosphate beads. *Journal of Applied Polymer Science* 134 (46), 45511.

Guibal E. (2004). Interactions of metal ions with chitosan-based sorbents: a review. *Separation and Purification Technology* 38, pp. 43–74.

Guibal E., Dambies L., Guimon C. and Yiacoumi S. (2001). Characterization of metal ion interactions with chitosan by X-ray photoelectron spectroscopy. *Colloids Surf. A* 177, pp 203–214.

Jean Y.C., Mallon P.E. and Schader D.M. (Eds.) (2003). Principles and Applications of Positron and Positronium Chemistry. World Scientific Publishing Co. Pte. Ltd., Singapore. ISBN: 981-238-144-9.

Jean Y.C. (1990). Positron annihilation spectroscopy for chemical analysis: a novel probe for microstructural analysis of polymers. *Microchemical Journal*, 42, 72.

Jiang X., Chen L. & Zhong W. (2003). A new linear potentiometric titration method for the determination of deacetylation degree of chitosan. *Carbohydrate Polymers*, 54, 457–463.

Johnson L.W and McGlynn S.P. (1970). The electronic absorption spectrum of chromate ion. *Chemical Physics Letters* 7 (6), pp 618-620.

Krajewska B. (2001). Diffusion of metal ions through gel chitosan membranes. *Reactive & Functional Polymers* 47, pp 37–47.

Kyzas G., Kostoglou M. and Lazaridis N. (2009). Copper and chromium (VI) removal by chitosan derivatives-Equilibrium and kinetic studies. *Chemical Engineering Journal* 152, pp 440-448.

Li A., Lin R., Lin C., He B., Zheng T., Lu L, Cao, Y. (2016). An environment-friendly and multi-functional absorbent from chitosan for organic pollutants and heavy metal ion. *Carbohydrate Polymers* 148, pp 272-280.

Lü R., Cao Z., Shen G. (2008). Comparative study on interaction between copper (II) and chitin/chitosan by density functional calculation. *J. Mol. Struct.: THEOCHEM* 860, pp 80–85.

McCullagh C., Yu Z., Jamieson A., Blackwell J. and McGerve J. (1995). Positron Annihilation Lifetime Measurements of Free Volume in wholly Aromatic Copolyesters and Blends. *Macromolecules* 28, pp 6100-6107.

Muzzarelli R.A.A. (1973). Natural Chelating Polymers, Pergamon Press, Oxford.

Nakanishi H., Wang S.J. & Jean Y.C. (1988). Microscopic surface tension studied by positron annihilation. In S. C. Sharma (Ed.), Positron annihilation studies of fluids (pp. 292–298). World Scientific Publishing Co. Pte. Ltd., Singapore.

Nithya R., Gomathi T., Sudha P., Venkatesan J., Anil S., Kim S-K. (2016). Removal of Cr(VI) from aqueous solution using chitosan-g-poly(butylacrylate)/silica gel nanocomposite. *International Journal of Biological Macromolecules* 87, pp 545–554.

Ogawa K., Oka K., Yui T. (1993). X-ray study of chitosan-transition metal complexes. *Chemistry of Materials* 5, pp. 726-728.

Olivera S., Muralidhara H.B., Venkatesh K., Guna V.K., Gopalakrishna K., Kumar K.Y. (2016). Potential applications of cellulose and chitosan nanoparticles/composites in wastewater treatment: A review. *Carbohydrate Polymers* 153, pp 600-618.

Qin C., Du Y., Zhang Z., Liu Y., Xiao L. and Shi X. (2003). Adsorption of chromium (VI) on a novel quaternized chitosan resin. Journal of Applied Polymer Science 90(2), pp 505-510.

Ray L., Galy J., Sautereau H, Simon G. and Cook W. (2004). PALS free volume and mechanical properties in dimethacrylate-based thermosets. *Polymer International* 53 (5), pp 557–56.

Rhazi M., Desbrieres J., Tolaimate A., Rinaudo M., Vottero P., Alagui A., El Meray M. (2002). Influence of the nature of the metal ions on the complexation with chitosan. Application to the treatment of liquid waste. *European Polymer Journal* 38, 1523–1530.

Rinaudo M. (2006). Chitin and chitosan: properties and applications. *Progress in Polymer Science*, 31, 603–632.

Schlick S. (1986). Binding Sites of Cu^{2+} in Chitin and Chitosan. An Electron Spin Resonance Study. *Macromolecules* 19, pp. 192-195.

Schmuhl R., Krieg H., Keizer K. (2001). Adsorption of Cu(II) and Cr(VI) ions by chitosan: Kinetics and equilibrium studies. *Water SA* 27(1), pp 1-7.

Shen C., Chen H., Wu S., Wen Y., Li L., Jiang Z., Li M., Liu W. (2013). Highly efficient detoxification of Cr(VI) by chitosan–Fe(III) complex: Process and mechanism studies. *Journal of Hazardous Materials* 244– 245, pp 689– 697.

Skorik Y.A., Gomes C.A.R., Podberezskaya N.V., Romanenko G.V., Pinto L.F., Yatluk Y.G. (2005). Complexation models of N-(2-Carboxyethyl) chitosans with Copper (II) ions. *Biomacromolecules* 6(1), 189-195.

Tao S.J. (1972). Positronium annihilation in molecular substances. *Journal of Chemical Physics* 56, 5499–5510.

Terreux R., Domard M., Viton C., Domard A. (2006). Interactions Study between the Copper II Ion and Constitutive Elements of Chitosan Structure by DFT Calculation. *Biomacromolecules* 7, 31-37.

Tirkistani F.A.A. (1998). Thermal analysis of some chitosan Schiff bases. *Polymer Degradation and Stability* 60, pp. 67-78

Trimukhe K. and Varma A. (2009). Metal complexes of crosslinked chitosans: Correlations between metal ion complexation values and thermal properties. *Carbohydrate Polymers* 75(1), pp. 63-70.

Trimukhe K.D. and Varma, A.J. (2008). A morphological study of heavy metal complexes of chitosan and crosslinked chitosans by SEM and WAXRD. *Carbohydrate Polymers* 71, 698-702.

Vieira R., Meneghetti E., Baroni P, Guibal E, González de la Cruz V., Caballero A., Rodríguez-Castellón E., Beppu M. (2014). Chromium removal on chitosan-based sorbents - An EXAFS/XANES investigation of mechanism. *Materials Chemistry and Physics* 146, pp 412-417.

Wilkins R.G (Ed.) (2002). A Survey of the Transition Elements - Chapter 8. In *Kinetics and Mechanism of Reactions of Transition Metal Complexes*, 2nd Edition. Wiley.

Xia R., Cao X., Gao M., Zhang P., Zeng M., Wang B., Wei L. (2016). Probing sub-nano level molecular packing and correlated positron annihilation characteristics of ionic cross-linked chitosan membranes using positron annihilation spectroscopy. *Physical Chemistry Chemical Physics* 19(5), pp. 3616-3626.

Zekriardehani S., Jabarin S., Gidley D., Coleman M. (2017). Effect of chain dynamics, crystallinity, and free volume on the barrier properties of poly(ethylene terephthalate) biaxially oriented films. *Macromolecules* 50(7), pp. 2845-2855.